NASA Technical Memorandum 81163

An Extended Soft-Cube Model for the Thermal Accommodation of Gas Atoms on Solid Surfaces

John R. Burke and D. J. Hollenbach

January 1980

National Aeronautics and
Space Administration

NASA Technical Memorandum 81163

An Extended Soft-Cube Model for the Thermal Accommodation of Gas Atoms on Solid Surfaces

John R. Burke, San Francisco State University, San Francisco, California
D. J. Hollenbach, Ames Research Center, Moffett Field, California

National Aeronautics and
Space Administration

Ames Research Center
Moffett Field, California 94035

AN EXTENDED SOFT-CUBE MODEL FOR THE THERMAL ACCOMMODATION OF GAS ATOMS ON SOLID SURFACES

JOHN R. BURKE

Department of Physics and Astronomy, San Francisco State University, San Francisco, California 94132, USA

and

D. J. HOLLENBACH

Ames Research Center, NASA, Moffett Field, California 94035, USA

Received _____

A numerical soft-cube model is developed for calculating thermal accommodation coefficients α and trapping fractions f_t for the interaction of gases incident upon solid surfaces. This model extends previous work by introducing a semiempirical correction factor c which allows the calculation of α and f_t when the collision times are long compared to the surface oscillator period, and by treating the processes of trapping, evaporation, and detailed balancing more accurately. The numerical method is designed to treat economically and with moderate (±20%) accuracy the dependence of α and f_t on finite and different surface and gas temperatures for a large number of gas/surface combinations. Comparison is made with experiments of rare gases on tungsten and on alkalis, as well as one astrophysical case of H_2 on graphite. The dependence of α on the soft-cube dimensionless parameters is presented graphically.

1. Introduction

Two parameters of particular interest to astrophysicists, as well as surface scientists, are the thermal energy accommodation coefficient α and the trapping fraction f_t of a gas at temperature T_g interacting with a solid surface at temperature T_s. These parameters are defined in terms of the flux of energy transferred from the gas to the surface F_e and the flux of gas molecules trapped on the surface F_t:

$$F_e = F_c\alpha(2kT_g - 2kT_s) \; ; \tag{1}$$

$$F_t = F_c f_t \; ; \tag{2}$$

where

$$F_c = nv_T/4 = n(kT_g/2\pi m_g)^{1/2} \tag{3}$$

is the flux of gas particles of number density n, thermal speed v_T, and mass m_g incident on the surface. The $2kT_g$ in eq. (1) is the average kinetic energy of a gas atom striking the surface.

Astrophysicists require values of α and f_t for the common interstellar gases H, H_2, He, C, N, O, CO, and H_2O incident on the surfaces of graphite, silicates and ices, which are thought to exist as tiny "dust" grains in interstellar space. Interstellar conditions generally produce a range of gas temperatures $10\ K < T_g < 10^4\ K$, surface temperatures $5\ K < T_s < 10^3\ K$, and gas densities $0.1 < n < 10^6\ cm^{-3}$. Since the radiation energy density is often equivalent to that of a blackbody near 3 K, the interstellar medium is far from thermal equilibrium and T_s is generally quite different from T_g. Values of α are therefore important in determining the gas-grain energy flow, which can dictate

the evolution of (and infrared emission from) interstellar clouds of gas and dust. The trapping fraction f_t is primarily important in interstellar chemistry, since the major mechanism for producing H_2 is initiated by trapping H atoms on grain surfaces; f_t also provides a measure of the depletion rate of heavier atoms and molecules from the interstellar gas onto the solid surfaces. Astrophysicists, therefore, require α and f_t for a wide range of gas temperatures, solid temperatures, and mass ratios

$$\mu = m_g/m_s \tag{4}$$

where m_s is the mass of a surface atom; however, their tolerance for error is large (up to a factor two) because of inherent uncertainties in the composition and roughness of the solid surface. The intent of this work is then to provide a practical means of computing accommodation coefficients and trapping fractions to the accuracy required by astrophysicists. In this paper we develop an extension of the original "soft-cube" model [1,2]. A subsequent paper will present results for astrophysical cases of interest.

The "soft-cube" model treats the gas/surface repulsive interaction as if the gas atom strikes a single surface atom which is attached by a single spring to a fixed lattice. The component of momentum parallel to the solid surface is assumed to be conserved for the gas atom during the interaction. Although this model ignores lattice and quantum mechanical effects, experimental values of α can be fitted rather well over a wide range of temperatures by fixing one dimensionless free parameter, assuming that the effective natural frequency, ω_e, of the surface oscillator, the range, b, of the repulsive force between gas atom and surface atom, and

the depth, D, of the attractive potential between surface and gas atom are known [3]. The advantage of the soft-cube model, as opposed to more exact lattice or quantum mechanical models, is that it is the simplest and most computationally economical method to treat the effects of finite and different surface and gas temperatures on α and f_t for a large number of gas/surface combinations.

The extended soft-cube model presented here improves upon previous work in several important respects. The original soft-cube model obtained an analytic result for the energy transfer in a single collision by assuming that the interaction can be treated as a short force pulse which peaks at the distance of closest approach of the gas atom to the surface atom [1]. These results are not valid when the collision time t_c is long compared with the surface oscillator period t_e, since there are then several (a number about equal to the ratio t_c/t_e) force pulses during the interaction. We have treated the collision by numerically integrating the trajectories of incident gas atoms, thereby extending the validity of the soft-cube model to regimes $t_c/t_e > 1$. As t_c/t_e increases, however, the lattice has an increasing effect on α and f_t which may not be ignored. These lattice effects may be included in the model approximately by reducing the effective oscillation frequency of the surface atom. If we write

$$\omega_e = c\omega_D \ , \tag{5}$$

where ω_D is the bulk Debye frequency of the solid, the lattice effects are then expressed by the correction factor c. From extensive comparisons with experimental data a semi-empirical relation is obtained for c

in terms of t_c/t_e that permits extension of the model to cases where experimental data are unavailable.

Secondly, an important effect of finite T_s is to permit "multiple collisions" even when $t_c/t_e < 1$. Physically, this can be pictured as the gas atom striking a surface atom which is oscillating into the surface, subsequently following the surface atom until it slows and/or reverses its motion, and finally making further collision(s) with the same surface atom. The original soft-cube model assumed all such multiple collisions lead to trapping [1]; by numerically integrating trajectories we can treat such multiple collisions exactly. Detailed balancing cannot be achieved unless multiple collisions are included realistically [4].

We have also treated the processes of trapping, evaporation and detailed balancing in more detail than most previous work. Previous assumptions generally dictated that an atom is trapped when its component of energy normal to the surface becomes negative [1,2,4]. In effect, this means that an atom hops along the surface until it dissipates its component of energy parallel to the surface. This overestimates the trapping probability if the "true" criterion is that the <u>total</u> energy of the incident atom must become negative [5,6]. The further assumption generally made is that a trapped atom eventually evaporates with $2kT_s$ of energy, having completely thermalized with the surface. Not only can hopping atoms be ejected from the surface prior to thermalization, but detailed balance dictates that even thermalized atoms evaporate with the average incident energy of the <u>trapped</u> atoms, which is <u>not</u> $2kT_s$ when $f_t < 1$ and $T_g = T_s$.

Section 2.1 briefly describes the extended soft-cube model, discussing the important parameters, and describing the computation of energy transfer in a single gas atom collision with a surface atom. The details of the computation are presented in appendix A. Section 2.2 develops the method used to handle trapping and evaporation. We distinguish two extreme criteria for trapping which allow investigation of the importance of hopping and surface roughness, and discuss the sensitivity of the trapping probability to the initial phase of the surface atom. Section 2.3 describes the numerical procedures used to average over gas and surface atom energy and surface atom initial phase. Details are presented in appendices B and C. The results are plotted in section 3 versus the experimental values. The quality of the extended soft-cube fits and the values of the correction factor c are compared to previous work. We find that the deviation of c from unity may be due to the effect of long collision times $t_c/t_e >> 1$, whereas previously it had been ascribed to surface effects. For some of the experimental data, values of D (the adsorption energy of a gas atom to the surface) are quite uncertain, providing a second "free" parameter. We discuss the most likely value of D in those cases using theoretical arguments as well as our best two-parameter fits. Section 3 concludes with a discussion of the dependence of α and f_t on all the physical parameters involved, focusing especially on the dependence of α with T_s. It has been assumed that α is independent of T_s, thereby facilitating theories of α which take $T_s = 0$. This assumption is critically analyzed in several recent reviews [2,7,8]. We find that the relation between α and T_s may in fact be quite complex,

particularly in the temperature range $kT_g \lesssim D \lesssim kT_s$. Finally, section 4 summarizes the significance of the results.

2. General description of the model

2.1 Microscopic interaction

The soft-cube approximation models the solid surface as in fig. 1 by an array of cubical atoms bound to the solid lattice by springs. An incoming gas atom, incident at angle θ, first encounters a collective attraction to the surface through a potential of depth D changing its incidence angle to θ', and then encounters a repulsive potential due to the individual surface atom with which it collides. The model assumes that forces between the surface and the impinging atom act normal to the surface, so that dynamically the problem reduces to one dimension.

The interaction potential between a gas atom and a surface atom is assumed to depend exponentially on their separation (cf. eq. (A1)). As is shown in appendix A, only this exponential form of the potential and its e-folding distance b are important; one need not specify the absolute value of the potential at any point or the exact value of the separation at which the gas atom reverses its motion.

The equations of motion for the two-atom system follow directly from Newton's Laws. Specification of initial and final conditions for the encounter completely determines the resulting energy transfer. The details of the procedure are found in appendix A; we mention here the most significant points.

Prior to the beginning of the interaction, the motion of the surface atom is taken to be that of an undisturbed harmonic oscillator:

$$R_s = R_o \sin(\omega_e t + \psi) , \qquad (6)$$

where R_s is the displacement of the surface atom from its equilibrium position; R_o is an amplitude related to the energy E_s of the surface atom, and ω_e is the effective oscillation frequency of the atom. The time t is taken to be zero at the beginning of the interaction, so that the angle ψ describes the initial phase of the surface atom. Since the arrival of gas atoms is timed randomly with respect to the motion of surface atoms, ψ is treated as a random variable.

The initial conditions for the gas atom are its speed and distance from the surface at the beginning of the encounter. The speed is of course given in terms of the part of the atom's original thermal energy in motion normal to the surface E_g augmented by the collective attractive potential energy of the surface D (i.e., the adsorption energy per atom).

The exact value of the initial atom-surface separation chosen is unimportant, though it must satisfy a few simple criteria. The exponential form of the potential calls for a formally infinite initial distance. In practice, one requires that the value of the potential at the initial point be small compared to gas atom energy, surface atom energy, or energy transfer. The condition for ending the computation is simply the return of the gas atom to this initial position.

As is shown in appendix A, the energy transfer, E_g, in a collision with given mass ratio μ is determined by four parameters: the collision parameter K given by

$$K = D/(2m_g\omega_e{}^2b^2) \ , \tag{7}$$

where b is the range of the Morse exponential repulsive potential; the ratio of initial gas speed to maximum speed of the undisturbed surface oscillator,

$$\zeta = v_o/R_o\omega_e = [(D + E_g)/\mu E_s]^{1/2} \ ; \tag{8}$$

the initial phase of the surface oscillator ψ; and a parameter ε equal to the square of the ratio of the oscillator period t_e to the collision time t_c,

$$\varepsilon = K(1 + E_g/D) = (t_e/t_c)^2 \ . \tag{9}$$

Equation (9) effectively defines the collision time t_c, which is approximately the time for an incident atom, accelerated by D, to traverse a distance b [9]. At fixed μ the functional dependence of the energy transfer ratio $\Delta E_g/D$ on ε, ζ, and ψ is implicit via integration of the equations of motion; the dependence of $\Delta E_g/D$ on K is explicitly given by eq. (A10).

2.2 Thermodynamic considerations

Several considerations arise when we look beyond the first collision an atom makes the surface. In the soft-cube model, only the motion of the gas atom perpendicular to the surface figures in an individual interaction; yet on average the gas atom has energy kT_g in its motion parallel to the surface. Should the gas atom emerge from its first collision still with positive energy in the perpendicular direction it will simply rebound, and its horizontal energy will be of no consequence

(dashed line in fig. 1). On the other hand, should it lose its incident normal energy in the first encounter, the gas atom will remain near the surface "hopping" from surface atom to surface atom and undergoing numerous subsequent energy transfers until it either escapes or is trapped on the surface. Hopping is thus defined as the process of moving horizontally across a surface with positive energy; trapping is defined as the process of attaining negative energy in the attractive potential well near the surface. A major thrust of this paper is to obtain information on the fraction of incoming gas atoms trapped by the surface. To do so, one ideally desires a detailed consideration of hopping, which we hope to include in subsequent research. For the present, however, we distinguish two limiting cases.

In the smooth surface (hereafter, hopping) case we suppose that subsequent hops slowly transfer initial horizontal energy to the surface. Thus, any atom which loses its perpendicular energy in the first collision hops across the surface until it is trapped. This limiting case ignores the possibility of escape after several hops. The opposite, rough surface, or "nonhopping" case assumes that the first collision is at an angle such that the rebounding atom emerges normal to the surface. In this case an atom may be said to be trapped only if it loses its <u>total</u> initial energy in the first collision.

Trapping is very sensitive to the phase of the surface atom at collision. One might suppose that trapping should occur only for the least energetic gas atoms; however, this view is completely incorrect when the surface has a finite temperature. Not only is it possible for surprisingly energetic atoms to be trapped at some phases ψ, but trapping can

increase for increasing surface temperature. This latter effect occurs when increased surface temperature produces a larger range of phase ψ in which the relative velocities of the gas and surface atoms at collision result in stopping and trapping the gas atom.

The dependence of the energy transfer in a single collision on phase is crucial for understanding detailed balancing and demonstrates the fallacy in attempting to define a single critical energy for trapping. Suppose that the gas and surface are at equal temperature and that only gas atoms with less than some critical energy are trapped. The phase-averaged energy transfers as a function of gas energy are fairly small but systematically biased toward gas to grain transfers, since the inward, collective, attractive potential D makes the average gas atom act as if it were a bit hotter than the surface. The net result of energy transfer by nontrapped atoms in such a phase-averaged model is an energy flow to the surface. Such a result contradicts the principle of detailed balance. What has gone wrong is that the actual energy transfers between individual gas and surface atoms are much larger in magnitude than their phase average. Some rather slow incoming gas atoms hit outward-moving surface atoms and are not trapped, leaving the surface with greatly increased energy; while some energetic atoms strike inward-moving surface atoms and leave with greatly decreased energy, or are trapped. Indeed, by accounting for the energetic atoms which are trapped as well as the slow atoms which rebound, detailed balancing of the nontrapped atoms can be achieved. As a check on this reasoning we replaced the exponential interaction potential with hard sphere collisions and found it possible to obtain results which exhibit detailed

balancing to very good precision (1 part in 10^4) over a wide range of parameters. Consequently, detailed balancing provides a check on the accuracy of the numerical schemes used to work with the more complicated exponential potential.

Evaporation of gas atoms from a surface, like hopping, is much too intricate to handle in detail. Nevertheless, the detailed balancing principle requires that ejection of trapped atoms from the surface exactly equal the trapping of atoms from the gas, when gas and surface temperatures are equal. By computing the average energy of atoms trapped at equal gas and surface temperature, we obtain the average energy of evaporated atoms at this surface temperature. When gas and surface temperatures are unequal, we assume that the average energy of evaporating atoms depends only on the surface temperature and not on the gas temperature. Furthermore, we assume that the number of atoms residing on the surface reaches equilibrium so that the rates of trapping and of evaporation are equal.

The mathematical details of the procedures outlined in this section may be found in appendix B.

2.3 Numerical procedures

The principle difficulty in using the extended soft-cube model is finding the appropriate compromise between numerical accuracy and computational expense. For a given gas/surface combination, the goal is the ability to calculate α and f_t efficiently over a wide range of T_s and T_g. Therefore, for fixed μ we have chosen to calculate the trajectories of gas atoms interacting with the surface for a three-dimensional grid

$(\psi, \varepsilon, \zeta)$ as discussed in appendix A. These results can then be used to interpolate the energy transfer $\Delta E_g/D$ in any collision of a gas atom with the surface (see eq. A10). Therefore, for any combination of T_g and T_s, a grid of energy transfers can be interpolated for the appropriate range of ψ, E_g, and E_s which can then be integrated numerically over a Maxwell-Boltzmann distribution to obtain α and f_t. Furthermore, for fixed T_g and T_s, α and f_t can be computed for a wide variation in the physical parameters D, b, and ω_e using the same trajectory grid. Herein lies the advantage over Monte Carlo schemes; once the $(\psi, \varepsilon, \zeta)$ trajectory grid is calculated for fixed μ, the accommodation coefficient and trapping fraction can be obtained for large ranges of T_g, T_s, D. b, and ω_e with little additional computational expense.

Numerical errors are introduced both in the coarseness of the trajectory grid from which we interpolate $\Delta E_g/D$ as a function of ψ, E_g, and E_s and in the coarseness of the subsequent grid used for the integration over ψ, E_g, and E_s for given T_g and T_s. As discussed in appendices B and C, we have chosen grid sizes which each introduce errors of about ±10%. Therefore, the numerical accuracy on the computations of α and f_t is within ±20%.

3. Results

3.1. Choice of parameters

The basic equations of motion (A5a) and (A5b) and the initial conditions (A9a-e) reveal that the average gas/surface energy transfer $\langle \Delta E_g \rangle$ for given T_g and T_s (eq. A10) and hence the classical sticking and accommodation coefficients are determined by the physical parameters μ, D,

ω_e, and b. In addition, the effective oscillator frequency ω_e appears only in the combination $\omega_e b$. The parameters μ and D are often known, whereas the appropriate $\omega_e b$ is somewhat more uncertain.

In order to match experiment, μ and D are assumed to be fixed and

$$\omega_e b = c\omega_D b \tag{11}$$

where c is an adjustable parameter and ω_D is the bulk Debye frequency. The original soft-cube model found for rare gases on tungsten that $c \simeq 1/2$ and deduced that therefore the appropriate oscillator frequency ω_e was approximately one-half the bulk Debye frequency [3], attributing this result to surface effects. The results presented in section 3.2, which cover a larger number of cases, reveal that $0.3 < c < 1$ and that c is a decreasing function of t_c/t_e. Since lattice models [7] for accommodation coefficients fit experiment with natural spring frequencies given by ω_D and since we obtain $\omega_e = \omega_D$ when $t_c < t_e$, it appears that deviations of c from unity occur when collision times are long, lattice effects become important, and the soft-cube model begins to fail. The sense of the correction is such that smaller values of c yield larger accommodation coefficients, as the longer collision times allow more of the lattice atoms to participate in the energy transfer.

Any conclusions about the dependence of c on t_c/t_e are based on the assumption that ω_D and b are known. The bulk Debye frequency is generally known to 5% accuracy, an estimate obtained by comparing the reported values of the last two decades [10-12]. However the range b of the Morse exponential repulsive potential is more uncertain since it is not measured directly but calculated from the combination rule and

values of b given for gas atom-gas atom and surface atom-surface atom interactions [13,14]. The accuracy of b for the gas atom-surface atom interaction can only be crudely estimated to be approximately ±30% from the span of determined values of b from 0.26 to 0.64 (see table 1).

The parameter D is taken to be the heat of adsorption. For those cases where the heat of adsorption is unknown, we take values of D from the literature. These values are calculated from crude extrapolations of known parameters and are often uncertain to factors of 2 to 4. For example, in Van der Waal theory of induced dipole-dipole interactions, the gas/surface potential well depth D_{gs} is proportional to the polarizability of the gas atom, or equivalently, to the square root of the potential well depth ε_{gg} for the gas atom-gas atom interaction. Values of ε_{gg} for rare gases [15] include $\varepsilon_{He-He} \simeq 8$ K, $\varepsilon_{Ne-Ne} \simeq 30$ K, $\varepsilon_{Ar-Ar} \simeq 120$ K, $\varepsilon_{Kr-Kr} \simeq 170$ K, and $\varepsilon_{Xe-Xe} \simeq 220$ K. (When numerically specifying ε_{gg} and D, we shall use the more intuitive temperature units rather than energy units.) Taking $D_{Ar-W} \simeq 1000$ K for argon on tungsten from the experimental heat of adsorption [16], we obtain from Van der Waal theory $D_{He-W} \simeq 260$ K, $D_{Ne-W} \simeq 500$ K, $D_{Kr-W} \simeq 1200$ K, and $D_{Xe-W} \simeq 1350$ K. The latter two conflict with the experimental heats of adsorption: $D_{Kr-W} \simeq 2250$ K and $D_{Xe-W} \simeq 4500$ K [16]. Extrapolating D_{He-W} and D_{Ne-W} from D_{Ar-W} by assuming D proportional to ε_{gg} obtains $D_{He-W} \simeq 60$ K and $D_{Ne-W} \simeq 200$ K, values more traditionally accepted in the literature [17]. On the other hand, $D_{Ne-W} = 350$ K and $D_{He-W} = 100$ K have been obtained as the values which, substituted into soft-cube theory, gives the best fit to measured accommodation coefficients [2,3]. Therefore, estimates for D_{He-W} and D_{Ne-W} range from 60 K to 260 K and 200 K to

500 K, respectively. Likewise, the potential well-depths for rare gases on the alkali metals are quite uncertain. Values for He on K range from $D_{He-K} \simeq 16$ K to 60 K [17,18]. Fortunately, the results are more sensitive to the value of $\omega_e b$ than the parameter D, and our approach is to present results for a range of D which is representative of the values quoted in the literature. For the astrophysical cases in which we are most interested, the heats of adsorption are known so that D is specified.

Table 1 presents the values of physical parameters $\theta_D = \hbar\omega_D/k$, b, μ and D which were used in calculating all reliably measured accommodation coefficients for various gas/surface combinations. In the following section which discusses fits to experiment, we shall use the more familiar θ_D instead of ω_D.

3.2 Comparison with experiment

The measured values of α for rare gases on tungsten are presently the most reliable because of the low level of impurities on the tungsten surface prior to the experiment [7]. For this reason and because values of b, θ_D, and D are relatively well established for most of the gas/surface combinations we make a careful and detailed comparison of the extended soft-cube theory to experiment for these cases. However, in comparing the results for rare gases on alkalis with experiment, a much coarser (and less expensive) numerical grid is used which reduces the numerical accuracy from ±20% to roughly ±40%. The coarser grid is justified by the increased uncertainties both in the experimental results and in the values of the parameters b and D.

Experimental values for the equilibrium accommodation coefficients for noble gases striking tungsten surfaces are presented in figs. 2 to 4 together with our computed fits. For these fits we assumed the "conventional" values of D discussed above and varied $c\theta_D b$. For each computed curve, we calculated a weighted sum of squared deviations from the experimental values. The data fall into three groups: measurements between 77.4 K and 303 K using the low-pressure method and groups both at lower and higher temperatures using the temperature-jump method. As the goal was to avoid gross disagreement with experiment in any of the three temperature ranges, each group was weighted equally. Thus in each group of data available for a given atomic species, we calculated an average squared difference between the computed and experimental accommodation coefficients and then summed these averages to obtain a final figure of merit for the value of $c\theta_D b$ used. The "best" fit then is that which minimizes this figure of merit.

Figure 2 presents experimental results for Ne/W and four calculated fits: two values of D_{Ne-W} for both the hopping and nonhopping cases. The hopping case with $D_{Ne-W} = 240$ K fits the intermediate range, though with noticeable deviations in the low temperature range. The hopping case with $D_{Ne-W} = 400$ K fits reasonably well in all three temperature ranges, though the very rapid rise of the experimental data at low temperatures seems to elude the soft-cube model. The best fits for the nonhopping cases with $D_{Ne-W} = 240$ K and 400 K are also presented and do not simulate the overall behavior of α. Attempts to match nonhopping cases to the other rare gases on tungsten also provided similarly poorer fits than the hopping cases. Apparently, the

hopping criterion used is closer to the physical situation and hopping must be included in modeling accommodation coefficients and trapping fractions. In all models presented henceforth the hopping case will be used exclusively.

Figure 3 presents the results for helium (^{4}He) striking tungsten. The computed curve for $D_{He-W} = 60$ K and $c\theta_D b = 60$ KÅ reproduces the minimum in the experimental data near $T_g = T_s = 50$ K remarkably well, though the comparison in the middle range of temperatures is slightly outside our 20% estimated numerical error. All of the computed curves exhibit a lower slope at high temperatures than does the experimental data. As the interaction at high temperature should approach the limit given by a free particle interaction, which gives a constant accommodation coefficient, one might perhaps be skeptical of the experimental result at 600 K. The very sharp minimum at $T_s \simeq 50$ K may also be an artifact of fitting temperature jump measurements ($T_s < 40$ K) with low-pressure measurements ($T_s > 77$ K). If one optimizes the fit to the data from the low-pressure method and ignores the other temperature ranges, it is possible to improve the fit greatly in the middle range. The best fit is then for $D_{He-W} = 100$ K and $c\theta_D b = 73$ KÅ.

Also plotted in fig. 3 is a computed curve for ^{3}He striking tungsten using the same parameters as the best overall fits for ^{4}He. The arrows give experimental values for the difference between ^{3}He and ^{4}He. The results are quite consistent in the intermediate temperature range but diverge substantially at $T_s \simeq 50$ K for $D_{He-W} = 60$ K and $c\theta_D b = 60$ KÅ. Again $D_{He-W} = 100$ K and $c\theta_D b = 73$ KÅ provides the better fit to the relative accommodation coefficients for ^{3}He and ^{4}He on tungsten.

Results for Ar, Kr, and Xe are presented in fig. 4. The same general behavior appears as for the lighter gases. Our results fall roughly within 20% of experimental values and generally do not reproduce the steep slope of the experimental data at low temperatures. Xenon apparently is an exception to this rule.

Table 2 presents a comparison of some computed nonequilibrium accommodation coefficients with experiments. Here the parameter values are those from the previous fits to the equilibrium data. In general, the computed values are somewhat higher than the experimental results (typically, though, by an amount less than the sum of variation in the experimental values and the 20% computational uncertainty). One could improve the fit by varying parameter values slightly; we are mainly interested, however, in the dependence on T_s. The agreement for nonequilibrium data at three times higher surface temperatures than for the equilibrium data further substantiates the utility of the model.

The effect of varying D provides modest improvement for He and Ne on tungsten if we increase D from the "canonical" values of $D_{He-W} = 60$ K and $D_{Ne-W} = 240$ K to $D_{He-W} = 100$ K and $D_{Ne-W} = 400$ K, respectively. However, no improvement in the quality of the fit can be made by changing D for the other rare gases on tungsten. Since D_{He-W} and D_{Ne-W} are not experimentally established and quite uncertain, we suggest that the accommodation results imply higher values of D for these two cases than the "canonical" ones.

Comparison of these extended soft-cube results to the results of the original soft-cube model [1,3] shows very similar behavior; a good fit to experiment in the middle temperature range, some trouble fitting the

dip in experimental values for helium near 50 K, and inability to reproduce the steep slope of the experimental data at low temperatures. Both models fit xenon rather well. These features then seem to be inherent in the soft-cube model and not due, for example, to numerical error in our calculations.

Although the qualitative behavior of all soft-cube models is identical, the extended soft-cube model requires significantly lower values for the combination $c\theta_D b$ than previous soft-cube models [3]. Since the ratio of collision time to surface oscillator period for much of the temperature and parameter range in the experimental data and in the astrophysical case of interest is near the limit of validity of previous work ($t_c/t_e \simeq 3$), we believe the parameter choices from the exact numerical calculation are more reliable for use in calculating the dependence of c on t_c/t_e.

We have also applied the extended soft-cube model to the case of noble gases incident on various alkali metal surfaces, in order to understand further the dependence of effective surface frequency on the parameter t_c/t_e. Unfortunately, the values of surface potentials D are not nearly so well known as for the tungsten surface, and experiments have not been performed over so wide a range of temperatures as for tungsten. Furthermore, the experimental results (reviewed recently in the literature [7]) are substantially more uncertain than those we have used for tungsten. Given these uncertainties, the numerical grid fineness was correspondingly relaxed, increasing the numerical errors to ±40%. The resulting values of α from the extended soft-cube model are seen in table 3 to fit experimental results within the numerical error.

The uncertainty in the choice of effective oscillator frequency (or equivalently the correction factor c) for these cases arises chiefly from uncertainty in D rather than from the numerical errors.

3.3. Determination of the correction factor c

The correction factor c attempts to compensate for all the inaccuracies of the extended soft-cube model. The most important inaccuracies are the following: (i) the surface oscillator frequency may in fact be smaller than the bulk Debye frequency [1]; (ii) the lattice effects are important when $t_c/t_e > 1$; and (iii) the lattice effects are important when $\mu \gtrsim 1$.

Figures 5a and 5b present the dependence of c on t_c/t_e. For each combination of gas and surface species we calculate c and its probable error from the value of $c\theta_D b$ corresponding to the best fit to experiment and from the range of values for b and θ_D found in the literature. Similarly we compute central values and ranges for the ratio t_c/t_e using eq. (9). Since the quantity E_g, the thermal energy of impinging gas atoms, appears in the formula for t_c/t_e, we present graphs for two values of E_g. The results show substantial scatter about what is, nevertheless, a reasonably well-defined relation. The correction factor c is of order unity for $t_c/t_e < 1$ and c monotonically decreases with increasing collision time. The trend levels off for very large t_c so that the relatively large uncertainties in t_c/t_e for noble gases on tungsten do not noticeably affect the results. That $c \simeq 1$ for $t_c/t_e < 1$ indicates that the surface oscillator frequency can be taken to be the Debye frequency in this case and that the effective oscillator frequency (or $c\theta_D b$

in the soft-cube model drops because of lattice effects when $t_c/t_e > 1$. The dependence on gas energy is weak and makes little change in the form of the relation.

Figure 5c presents a similar plot of correction factor versus mass ratio μ. No correlation is seen for $\mu \lesssim 0.8$. Furthermore, in attempting to match experiment for cases such as the heavier rare gases on alkalis where $\mu > 1$, we find the extended soft-cube model cannot be made to match experiment for any value of c, in the sense that the experimental result is always higher than the theoretical value. Changing the effective oscillator frequency cannot imitate the effect of the lattice when a very massive gas atom strikes a light surface atom. Therefore, we assume that the correction factor c depends only on t_c/t_e but is valid only for $\mu \lesssim 0.8$; and that the effective oscillator frequency is ω_D when $t_c/t_e < 1$.

3.4. Application of the extended soft-cube model: an astrophysical case

As an interesting example of how the extended soft-cube model is to be used, consider the gas/surface combination: H_2/graphite. Here some experimental data are available for accommodation coefficients [19]; the values of $D = 525$ K [9,20] and $\theta_D = 420$ K [10] are known; and $b \simeq 0.3$ Å has been estimated [21]. We obtain a value $t_c/t_e = 1.24$ from equation (9) and therefore a value $c = 0.92$ from fig. 5.

Figure 6 presents the resulting values for the accommodation coefficient and trapping fraction computed from the extended soft-cube model. Since c is determined from t_c/t_e, the theory has no adjustable parameters and still fits the experimental points quite well. The worst

match is at 77 K, where the theoretical point lies 30% below the experimental value.

Although trapping fractions are difficult to measure experimentally, and few reliable results are available, the trapping fraction f_t for H_2 on graphite is plotted as well because it is of astrophysical interest, and because it illustrates a common relationship between α and f_t. At low temperatures, $f_t \simeq 1$ and the accommodation coefficient $\alpha \simeq 1$, as the gas atoms are trapped and re-evaporated with complete accommodation. At high temperatures $f_t \simeq 0$, but the accommodation coefficient $\alpha \simeq 2\mu/(1 + \mu)^2$ as partial accommodation is achieved by the richocheting gas atoms depositing the free-particle energy transfer to the surface atoms.

3.5. Investigation of parameter space

The dependence of α on the independent parameters of the model is complicated by the effects of trapping and the transition from free-particle interaction when $t_c/t_e < 1$ to lattice interaction when $t_c/t_e > 1$. The independent parameters enter the calculations as the mass ratio μ, the combination K defined in equation (7), and the ratios T_g/D and T_s/D.

From the μ dependence of the energy transfer in the collision of two free particles $\Delta E_g \propto \mu/(1 + \mu)^2$, the accommodation coefficients are expected to increase monotonically with μ for $\mu < 1$. K is proportional, approximately, to $(t_e/t_c)^2$; and, therefore, larger K generally means larger α, since more energy is transferred in a short collision time than in a long, more adiabatic one. Generally, α increases as T_g/D

decreases, since trapping becomes more important for $T_g/D < 1$. The dependence of α on T_s/D is not intuitively obvious, although some authors have argued that α is independent of T_s/D, particularly when trapping is not important and $T_s > T_g$ [7,8,22,23].

Figure 7 gives the dependence of α on mass ratio μ. The main feature is a monotonic increase of α with increasing mass ratio. Near $\mu \simeq 0.8$ however, the curves apparently reach a peak. Such behavior is reminiscent of the result for free-particle collisions, which peaks at $\mu = 1$, and is a symptom of building the model on single-particle encounters while neglecting lattice effects. We restrict the extended soft-cube model to values $\mu \lesssim 0.8$ in order to avoid major lattice effects caused by high μ.

Figure 8 gives the dependence of α on K. Smaller values of K correspond to larger t_c/t_e or, more crudely, to collisions in which the spring is relatively more important. Smaller K is also seen in fig. 8 to correspond in general to smaller values of the accommodation coefficient. In the limit $K = 0$ ($\omega_e = \infty$) the incoming particle strikes a surface atom rigidly attached to the solid. The system is conservative, and no energy transfer occurs.

The dependence of α on K can also be seen in fig. 7, where the importance of trapping is illustrated. The above argument suggests that a free-particle, hard-sphere limit ($t_c = 0$; $K = \infty$) might provide an upper limit to α. Trapping, however, drives α toward 1, and it is the dominant process for the large values of K in the temperature range represented. Notice also that curves for fixed K but increasing gas temperature in general lie lower in fig. 8, an effect caused by the

decrease in the trapping fraction as the gas temperature increases. The curves for $K = 0.1$ and $\mu = 0.11$, show an exception to this rule at $T_g/D \sim 1$. Here trapping is no longer important and the decrease in t_c/t_e (see eq. (9)) at the higher temperature leads to greater energy transfer in the richocheting gas atoms.

Further examples of the complexity of the behavior of α occur in figs. 9a and b, which display two cases of the variation of α with surface temperature. For most cases, the dependence is not large and it is customary in the literature [2,7,8] to take this as the general case. However, substantial variation of α with T_s occurs in some limiting cases. In particular, α increases with increasing surface temperature for $\mu \lesssim 0.1$, $K \lesssim 0.3$, and $T_g/D \lesssim 1$; α decreases with increasing surface temperature for $\mu \gtrsim 0.1$, $K \gtrsim 0.3$, and $T_g/D \lesssim 1$. The primary cause of this behavior is the variation of the trapping fraction, which may increase or decrease with surface temperature depending on the match of oscillator velocities to gas-atom velocities. The dependence of α on T_s is less pronounced or absent when $T_g/D \gtrsim 1.0$, when trapping plays a less significant role in determining α. This has been observed by other authors [22,23].

4. Discussion and conclusion

The goal of this work has been to construct a theoretical model of the gas/surface interaction which will provide approximate trapping fractions and thermal accommodation coefficients for gas/surface combinations which have not been studied experimentally. In particular, the astrophysical combinations of hydrogen and helium gases incident upon

graphite, silicate, or ice surfaces will be the subject of a future paper which will apply the basic method described here. A primary requirement of the model is the ability to treat finite surface temperature and "nonequilibrium" ($T_g \neq T_s$) effects.

To this end we have extended the analysis of the original soft-cube model [1], a model designed to handle surface temperature effects. The basic features of a soft-cube model are the following: (i) the surface atoms can be represented as independent one-dimensional oscillators connected by springs to an infinite mass substrate; (ii) a gas atom is accelerated by the long-range attraction adsorption potential D and interacts with a single-surface atom via a "soft" exponential repulsive potential; (iii) the surface atom is "cubical" in the sense that the tangential component of the gas atom is conserved in the interaction; and (iv) the surface atoms have an equilibrium energy distribution at the temperature of the solid. The fundamental assumptions of soft-cube models and the particular way they are treated in the extended soft-cube model include:

(1) The lattice can be ignored. This assumption strictly holds for $t_c/t_e \ll 1$ and $\mu \ll 1$. In the extended soft-cube model a correction factor c is applied to approximate the contribution of the lattice when $t_c/t_e > 1$. The dependence of c on t_c/t_e in the range $t_c/t_e < 5$, is found empirically by matching the results of the theory to experimental data. Furthermore, the theory reproduces observed accommodation coefficients for $\mu \lesssim 0.8$ but fails for larger μ as lattice effects

again begin to dominate. It proves impossible to construct a similar correction factor for high μ cases.

(2) The effect of surface roughness is small. Structural scattering becomes important when $T_g/D > 10$ [24]. Therefore, this assumption restricts the range of validity of a soft-cube model to $T_g \lesssim 500$ K for He on W, for example.

(3) Quantum mechanical effects are small. The analysis strictly holds for $T_g > \theta_D$ and for de Broglie wavelengths of the incident atoms small compared to the lattice spacing ($E_g/k \gtrsim 30$ K for He). Nevertheless, classical models provide surprisingly accurate fits to experiment when these conditions are violated [7].

(4) After the initial collision with a single-surface oscillator, the interaction of the gas atom with the surface can be approximated in a simple yet realistic manner. This interaction includes striking a second surface oscillator during the collision time, hopping across the surface, and trapping with consequent evaporation. The first effect is probably negligible [1]. The extended soft-cube model proposes two extreme criteria for hopping and trapping; either an atom is trapped if its component of energy normal to the surface becomes negative after the initial collision (hopping implied) or an atom is trapped only if its total energy becomes negative after the initial collision (no hopping). The hopping case allows a better match to experiment. Detailed balancing is used as a tool to estimate the average energy of an atom evaporating from a surface

at temperature T_s; it is taken to be equal to the average energy of an incident atom which is trapped when $T_g = T_s$. It is important to note that this average energy is <u>not</u> $2kT_s$ when $f_t < 1$, as has often been assumed.

The extended soft-cube model yields dependences of α on T_g and T_s which closely match experiment. Like the earlier soft-cube models [2], however, the model slopes are somewhat more positive than the experimental results. We obtain theoretical values within 25% of the experimental values over the entire temperature range for rare gases on W. In turn, the best theoretical fits for the various gas/surface combinations, including rare gases on alkalis, provide an empirical correction factor for lattice effects when $t_c/t_e > 1$. Given the dependence of the correction factor c on t_c/t_e, the model has no free parameters and predicts α and f_t given m_g, m_s, T_g, T_s, b, D, and ω_D (or θ_D). To check the goal of this work, namely to provide approximate values of α and f_t for astrophysical combinations, we have applied the extended soft-cube model to H_2 gas incident upon graphite, the only astrophysical case with experimental results available. Although b is not well determined, the previously estimated value of b [21] for this combination results in a theoretical fit to experiment within ~30%. This is well within the desired astrophysical accuracy of a factor of two. A future paper will apply the extended soft-cube model by calculating α and f_t for other astrophysical gas/surface combinations.

Acknowledgments

This work was supported in part by National Science Foundation Grants numbers AST 74-17362, AST 75-02181, and AST 77-23069. One of us (DJH) acknowledges the support of the National Research Council in the form of a Senior Associateship.

Appendix A

Equations of motion for the microscopic interaction

We take the interaction potential U between a gas atom and surface atom to be of the form

$$U = U_o \exp(-\rho/b) \tag{A1}$$

The distance ρ is the separation of the two atoms as shown in fig. 10; b is the e-folding scale of the potential. We shall show that the value of U_o need not be specified to solve for the energy transfer.

From Newton's Laws, we obtain

$$m_s\ddot{R}_s = -m_s\omega_e^2 R_s - (U_o/b)\exp(-\rho/b) \ , \tag{A2}$$

and

$$m_g(\ddot{R}_s + \ddot{\rho}) = (U_o/b)\exp(-\rho/b) \tag{A3}$$

where R_s is the displacement of the surface atom from its equilibrium position, and ω_e is the effective oscillator frequency.

One may put the equations into a more convenient form with the following abbreviations:

$$K = D/(2m_g\omega_e^2 b^2) \ , \tag{A4a}$$

$$\eta = R_s/b \ , \tag{A4b}$$

$$\chi = \rho/b + \ell n(D/2KU_o) \ , \tag{A4c}$$

and

$$\tau = \omega_e t \ . \tag{A4d}$$

One obtains

$$\eta'' = -\eta - \mu e^{-\chi} \tag{A5a}$$

and

$$\chi'' = \eta + (1 + \mu)e^{-\chi} , \tag{A5b}$$

where $'$ stands for the derivative with respect to τ. The parameter η is the dimensionless position of the surface atom while χ is a dimensionless measure of the distance between surface atom and gas atom.

Equations (A5a) and (A5b) may be solved numerically, once the initial conditions are specified. Thus, we take the motion of the surface atom before the beginning of the collision to be that of an undisturbed harmonic oscillator with position

$$R_s = R_o \sin(\tau + \psi) \tag{A6a}$$

and velocity

$$\dot{R}_s = \omega_e R_o \cos(\tau + \psi) \tag{A6b}$$

Here the phase ψ is a random variable giving the phase of oscillation when a collision begins. The initial speed of the gas atom is given in terms of its initial energy in motion normal to the surface, augmented by the collective potential D:

$$v_o = [2(D + E_g)/m_g]^{1/2} \tag{A7}$$

It proves convenient at this point to introduce the abbreviations

$$\zeta = v_o/R_o\omega_e = [(D + E_g)/\mu E_s]^{1/2} ; \tag{A8a}$$

$$\gamma = E_s/D ; \tag{A8b}$$

$$\beta = E_g/D \ ; \tag{A8c}$$

and

$$\varepsilon = K(1 + \beta) \ . \tag{A8d}$$

In terms of these quantities, the initial conditions read:

$$\eta_i = 2(\varepsilon^{1/2}/\zeta)\sin \psi \tag{A9a}$$

$$\eta_i' = 2(\varepsilon^{1/2}/\zeta)\cos \psi \tag{A9b}$$

and

$$\chi_i' = -2(\varepsilon^{1/2}/\zeta)(\zeta + \cos \psi) \tag{A9c}$$

There is no exact criterion for choosing χ_i. We shall require that the initial value of the interaction potential be much less than either the initial gas or grain energy,

$$\exp(-\chi_i) << \min(2\varepsilon, 2\varepsilon/\mu\zeta^2) \tag{A9d}$$

Furthermore, we choose χ_i so that the initial distance between the gas atom and the mean surface is independent of ψ. This allows a particularly simple averaging procedure over ψ since ψ will then be uniformly distributed. Specifically,

$$\chi_i = 4 + 2(\varepsilon^{1/2}/\zeta) + \max[0, -\ell n(2\varepsilon), -\ell n(2\varepsilon/\mu\zeta^2)] - \eta_i \tag{A9e}$$

The criterion for ending a numerical integration may simply be taken as the final value of χ being equal to the initial value. One then obtains the desired energy transfer ΔE_g between gas and surface atoms as the difference between final and initial energies of either gas or surface atom:

$$\Delta E_g/D = -(1 + \beta) + (\eta_f' + \chi_f')^2/4K$$
$$= \gamma - (\eta_f'^2 + \eta_f^2)/4\mu K \qquad \text{(A10)}$$

We note that the differential eqs. (A5), the initial conditions (A9), and energy transfer (A10) in their final forms make no reference to the quantity U_o, which describes the maximum interaction potential. As claimed above, the results depend only on the exponential form and e-folding distance b of the potential.

Comparison of eq. (A10) with eqs. (A8d-A9e) reveals that the energy transfer $\Delta E_g/D$ for fixed μ is set by the four parameters ε, ζ, ψ, and K. Furthermore, inspection of the eqs. of motion (A5a and b) along with the initial conditions (A9a, b, c, and e) shows that the integration of the trajectories for fixed μ is set by the three parameters ε, ζ, and ψ. Therefore, for fixed μ a complete three-dimensional grid $(\varepsilon, \zeta, \psi)$ of trajectories provides (via eq. (A10)) the energy transfer for any collision between a gas atom and a surface. In practice, a finite grid is used and interpolation is made to estimate the trajectories for any $(\varepsilon, \zeta, \psi)$ combination. We chose the coarseness of the $(\varepsilon, \zeta, \psi)$ grid so that interpolation errors lead to errors of less than 10% in f_t and α. Typically, the grid sizes were $24 \times 24 \times 20$, and typical ranges of ε and ζ were $0.05 \lesssim \varepsilon \lesssim 10$ and $1 < \zeta < 10^4$.

Appendix B

Definitions of α and f_t in terms of parameter distribution functions

We assume that the velocity distribution of gas atoms is given by the Maxwell-Boltzmann distribution. The flux of gas atoms from solid angle $d\Omega$ and velocity interval v to $v + dv$ above the attractive surface potential is

$$r(\theta,v)d\Omega\, dv = n(m_g/2\pi kT_g)^{3/2} \cos\theta\, d\Omega\, v^3 \exp(-m_g v^2/2kT_g)dv \qquad (B1)$$

where θ is the angle of incidence. All properties of the surface are assumed to be statistically isotropic in azimuthal angle about the normal.

We shall require the transformation of eq. (B1) to a distribution in terms of the variables θ', the polar angle at collision, and w, the total gas energy scaled according to gas temperature:

$$w = m_g v^2/2kT_g \qquad (B2)$$

Since the effect of the attractive potential is to leave the parallel energy of the atom unchanged while adding D to its normal energy, and the sines of angles θ and θ' are given by the ratio of parallel velocity to normal velocity, we may obtain:

$$\cos\theta = \{\cos^2\theta'[1 + (w\Theta_g)^{-1}] - (w\Theta_g)^{-1}\}^{1/2}\ , \qquad (B3)$$

where $\Theta_g = kT_g/D$ is a scaled gas temperature and Θ_s is the corresponding scaled surface temperature. We obtain the desired gas atom distribution function by substitution in eq. (B1) and multiplication by the Jacobian of the transformation:

$$r(w,\theta')dw\, d(\cos\theta') = -(nv_t/2\Theta_g)(1 + w\Theta_g)e^{-w}\, dw \cos\theta'\, d(\cos\theta') \qquad (B4)$$

Note that θ' is limited to the range

$$0 \leq \theta' \leq \cos^{-1}(1 + w\Theta_g)^{-1/2} = \theta_m(w) \tag{B5}$$

In the hopping case, defined in the text, the interesting parameter is energy in normal motion $E_\perp$ rather than total energy E_g. Thus, we require the distribution in terms of the variable

$$u = E_\perp/kT_g = E_g \cos^2 \theta/kT_g = w \cos^2 \theta = \cos^2 \theta'(w + \Theta_g^{-1}) - \Theta_g^{-1} \tag{B6}$$

Equation (B4) becomes

$$r(u,\theta')du\, d(\sec^2 \theta') = (nv_t/4\Theta_g)(1 + u\Theta_g)d(\sec^2 \theta')e^{-(u'+\Theta_g^{-1})\sec^2\theta'+\Theta_g^{-1}} \tag{B7}$$

with subsidiary condition

$$\theta \leq \theta' \leq \pi/2 \tag{B8}$$

The only feature of the hopping case which is not manifestly independent of the incidence angle is the energy transferred to the surface by atoms which are trapped. Each trapped atom is assumed to have the average transverse energy kT_g. Thus, we need only consider the distribution of atomic impacts averaged over angle and depending only on u:

$$r(u)du = \int_{\theta'=0}^{\pi/2} r(u,\theta')du\, d(\sec^2 \theta') = (nv_t/4)e^{-u}\, du \tag{B9}$$

For the distribution function of the energy of the surface atom we take the Boltzmann distribution

$$P(y)dy = e^{-y}\, dy \tag{B10}$$

where

$$y = E_s/kT_s \tag{B11}$$

These distributions for gas atoms (eq. (B4) for nonhopping and eq. (B9) for hopping) along with the surface atom distribution (B10) can be combined with the energy transfers and trapping criteria for one-dimensional collisions to define f_t and α.

The accommodation coefficient is defined as the ratio between the actual mean energy transfer per collision and that which would occur if each incoming atom were to be trapped, thermalized to the surface temperature, and then evaporated;

$$\alpha = \langle \Delta E_g \rangle / 2k(T_s - T_g) = 1/2 \langle \Delta E_g / D \rangle / (\Theta_s - \Theta_g) \tag{B12}$$

where ΔE_g is the actual mean energy transfer; $2kT_g$ is the mean energy of gas atoms at temperature T_g striking a surface. Note that if every atom were to be trapped, then in equilibrium the average energy of evaporators must equal that of those impinging; therefore $2kT_s$ represents the mean energy of evaporators when all atoms are trapped.

There are three contributions to the average energy transfer: (i) energy transferred by rebounding atoms; (ii) energy transferred by those trapped; and (iii) energy added to the gas by trapped atoms evaporating.

$$\langle \Delta E_g / D \rangle \equiv \langle \delta E \rangle = \langle \delta E \rangle_r - \langle \delta E(T_g) \rangle_t + \langle \delta E(T_s) \rangle_t \tag{B13}$$

where the subscripts r and t refer to rebounders and trapped atoms respectively.

Explicit expressions for the average of a function g over the parameter space are

$$\langle g \rangle = \int_{\omega=0}^{\infty} \int_{\theta'=0}^{\theta_m(\omega)} \int_{v=0}^{\infty} \int_{\psi=-\pi}^{\pi} g \frac{d\psi}{2\pi} e^{-v} dv(\omega + \Theta_g^{-1}) e^{-\omega} d\omega \, d(-\cos^2 \theta') \tag{B14a}$$

for the nonhopping case, and

$$\langle g \rangle = \int_{u=0}^{\infty} \int_{v=0}^{\infty} \int_{\psi=-\pi}^{\pi} g \frac{d\psi}{2\pi} e^{-v} dv \, e^{-u} du \tag{B14b}$$

for the hopping case.

In order to perform the averaging processes (B14a) and (B14b) on the three contributions listed in eq. (B13), we define several quantities in words whose quantitative calculation is performed numerically:

$p_t \equiv$ probability of an atom being trapped by the surface after collision;

$\delta E_t \equiv$ scaled ($\div D$) energy transfer from gas to surface of a trapped atom;

$\delta E_r \equiv \delta E(1 - p_t)$ = mean energy transfer in a single collision by atoms which are not trapped.

Equations (B12), (B13), and (B14) may be now combined to obtain the accommodation coefficient,

$$\alpha = \frac{1}{2} (\Theta_s - \Theta_g)^{-1} \left\{ \langle \delta E_r \rangle - \langle p_t \delta E_t \rangle + \langle p_t \delta E_t \rangle_{\Theta_g = \Theta_s} \right\} \tag{B15}$$

and the fraction trapped,

$$f_t \doteq \langle p_t \rangle \tag{B16}$$

Finally, we derive an expression for the accommodation coefficient when the gas and surface temperatures are nearly equal, which is useful in overcoming numerical uncertainties of the extended soft-cube model under such conditions. Thermodynamics guarantees that $\langle \delta E_g \rangle$ will vanish

for equal temperatures, so that the first term in a Taylor's expansion of $\langle \delta E_g \rangle$ obtains

$$\alpha(\Theta_g \simeq \Theta_s) = -\frac{1}{2}\left(\frac{\partial}{\partial \Theta_g}\right)\langle \delta E \rangle_{\Theta_g = \Theta_s} \tag{B17}$$

Appendix C

Numerical integrations over thermal distributions

For the integrations over gas and surface energy distributions we compared three methods: (i) direct integration via Simpson's rule; (ii) Gaussian quadrature; and (iii) Simpson's rule after a transformation of the form:

$$\int_0^\infty e^{-x} f(x)dx \rightarrow \int_0^1 f(-\ell n\ z)dz \tag{C1}$$

With the third procedure, which proved the most accurate, one must choose a value of the lower limit (equivalent to choosing how far out on the Maxwell tail to integrate) as well as the fineness of partition of the integration interval. A partition of 15 points each for gas and surface energy variables evenly spaced between 1 and 3×10^{-3} proved adequate. To compare the relative accuracy of different integration procedures we used a variant of the computer code which employs analytic results from the hard-sphere potential approximation to single encounters. For this case one may show analytically that detailed balance is satisfied, and the lack of errors in the single encounters thus provides a very sensitive test of the accuracy of the subsequent numerical techniques. With

the procedure described above, we were able to obtain an accuracy in this step of 1 part in 10^4.

The integration over phase angle also required care, since the trapping of an impinging gas atom is very sensitive to phase. Furthermore, the trapped and untrapped atoms must be handled separately, resulting in integration over grids with many zero entries. In this situation, the trapezoidal rule proved more accurate than Simpson's rule. We tested the dependence of the results on the fineness of the phase grid, using both the results of sensitivity to fineness and the detailed balancing check. A grid of 20 points kept errors to less than 10%.

Since the probability of trapping a gas atom varies greatly over the parameter space of interest, there were some cases with significant trapping only for the lowest gas energy grid point. In this case, any of the standard integration methods seriously overestimate the importance of trapping when, though small, it is still a significant contribution to the total energy transfer. In this case one may make use of the near constancy of the energy transfer and the Boltzmann distribution between the first two gas energy grid points to express the fraction trapped in terms of the ratio of energy transfer to the energy difference between the first two grid points.

With this refinement and the grid sizes mentioned above, our tests show the integrations accurate to about 10%, so that with the additional 10% inaccuracy due to interpolating in the grid of results for individual encounters (see appendix A) we expect an overall uncertainty in α and f_t to be 20%.

References

[1] R.M. Logan and J.C. Keck, J. Chem. Phys. 49 (1968) 860.

[2] F.O. Goodman, Surface Sci. 60 (1976) 45.

[3] R.M. Logan, Surface Sci. 15 (1969) 387.

[4] Ch. Steinbrüchel, Surface Sci. 66 (1977) 131.

[5] F.O. Goodman, in: 6th Intern. Symp. Rarified Gas Dynamics, Vol. 2, Eds. L. Trilling and H.Y. Wachman (Academic Press, New York, 1969) p. 1105.

[6] W.H. Weinberg and R.P. Merrill, J. Vacuum Sci. Technol. 10 (1973) 411.

[7] F.O. Goodman, Progr. Surface Sci. 5 (1974) 261.

[8] W.H. Weinberg, Advan. Colloid Interface Sci. 4 (1975) 301.

[9] D.J. Hollenbach and E.E. Salpeter, J. Chem. Phys. 33 (1970) 69.

[10] D. Gray (coordinating editor), American Institute of Physics Handbook (McGraw Hill, New York, 1972) p. 4-115.

[11] R.C. Weast (editor), Handbook of Chemistry and Physics (Chemical Rubber, 1977) D-169.

[12] C. Kittel, Introduction to Solid State Physics (Wiley, New York, 1971) p. 219.

[13] F.O. Goodman and H.Y. Wachman, J. Chem. Phys. 46 (1967) 2376.

[14] D.D. Konowalow and J.O. Hirschfelder, Phys. Fluids 4 (1961) 629.

[15] R.B. Bird, J.O. Hirschfelder, and C.F. Curtiss, in: Handbook of Physics, Eds. E.U. Condon and H. Odishaw (McGraw Hill, New York, 1958) Ch. 4-5, pp. 5-43.

[16] G. Ehrlich, in: Structure and Properties of Thin Films, Eds. Neugebauer, Newkirk, and Vermilyea (Wiley, New York, 1959) 451.

[17] L. Trilling, in: 5th Intern. Symp. Rarified Gas Dynamics, Vol. 1, Ed. C.L. Brundin (Academic Press, New York, 1967) p. 139.

[18] L. Trilling, Surface Sci. 21 (1970) 337.

[19] K.L. Day, in: IAU Symp. No. 52, Eds. J.M. Greenberg and H.C. VandeHulst (D. Reidel, Leiden, 1973) 311.

[20] G.C. Augason, Astrophys. J. 162 (1970) 463.

[21] D.J. Hollenbach, Center for Radiophysics and Space Research Report 338 (Cornell University, Ithaca, New York, 1969) 24.

[22] L.B. Thomas and E.B. Schofield, J. Chem. Phys. 23 (1955) 861.

[23] J. Kouptsidis and D. Menzel, Ber. Bunsen bes. Physik. Chem. 74 (1970) 512.

[24] R.A. Oman, J. Chem. Phys. 48 (1968) 3919.

[25] W. Watt and R. Moreton, R.A.E. (Farnborough) Tech. Note CPM 80 (1964).

[26] L.B. Thomas, in: 5th Intern. Symp. Rarified Gas Dynamics, Ed. C.L. Brundin (Academic Press, New York, 1967) 155.

[27] L.B. Thomas, in: Fundamentals of Gas Surface Interaction, Eds. H. Saltsburg, T.N. Smith, Jr., and M. Rogers (Academic Press, New York, 1967) 346.

[28] J. Kouptsidis and D. Menzel, Zeits. f. Naturforsch 24a (1969) 479.

[29] H.Y. Wachman, J. Chem. Phys. 45 (1966) 1532.

[30] D.V. Roach and L.B. Thomas, in: 5th Intern. Symp. Rarified Gas Dynamics, Ed. C.L. Brundin (Academic Press, New York, 1967) 163.

[31] G.L. Zweerink and D.V. Roach, Surface Sci. 41 (1974) 237.

Table 1

Gas surface interaction parameters

Gas/surface	μ	θ_D(K)[10]	b(Å)[13,14]	D(K)[3,13,16,17,18]
He^3/W	0.016	400	0.26	50 - 100
He^4/W	0.022	400	0.26	50 - 100
Ne/W	0.11	400	0.27	200 - 350
A/W	0.22	400	0.34	950
Kr/W	0.46	400	0.39	2250
Xe/W	0.71	400	0.40	4500
He/Li	0.58	370	0.5	20 - 60
He/Na	0.17	158	0.55	20 - 60
Ne/Na	0.88	158	0.56	40 - 200
He/K	0.10	90	0.63	20 - 60
Ne/K	0.52	90	0.64	40 - 200

Table 2

Nonequilibrium accommodation coefficients for helium and argon on tungsten

Ar/W: T_g = 303 K				
T_s	1073 K	1335 K	1558 K	1785 K
α(experimental) [25]	25 ± 5[a]	25 ± 6	22 ± 6	23 ± 7
α(D = 950 K, $c\theta_D b$ = 43 KÅ)	31	30	29	29
He/W: T_g = 77 K				
T_s	97 K	117 K	137 K	147 K
α(experimental) [23]	1.26	1.26	1.26	1.28
α(D = 60 K, $c\theta_D b$ = 60 KÅ)	1.04	1.09	1.15	1.15
α(D = 100 K, $c\theta_D b$ = 73 KÅ)	1.28	1.46	1.51	1.52
He/W: T_g = 303 K				
T_s	1073 K	1335 K	1558 K	1785 K
α(experimental) [25]	1.8 ± 0.2	1.8 ± 0.2	1.8 ± 0.2	1.8 ± 0.2
α(D = 60 K, $c\theta_D b$ = 60 KÅ	2.0	2.0	1.9	2.0
α(D = 100 K, $c\theta_D b$ = 73 KÅ	2.1	2.1	2.2	2.3

[a] All values of α are multiplied by 100.

Table 3

Equilibrium accommodation coefficients for rare gases on alkali metals

He/Li: T_s			83 K	193 K	273 K
	α(experimental) [26,27]		2.8[a]	4.7	6.0
	α(D = 20 K; $c\theta_D b$ = 80 KÅ)		2.0	8.1	10.0
	α(D = 60 K; $c\theta_D b$ = 100 KÅ)		1.6	5.2	7.1
He/Na: T_s		78 K	90 K	195 K	298 K
	α(experimental) [26,27]	3.5	3.8	6.5	9
	α(D = 20 K; $c\theta_D b$ = 60 KÅ)	2.9	4.6	7.4	10.3
	α(D = 60 K; $c\theta_D b$ = 70 KÅ)	4.1	3.8	8.4	11.0
He/K: T_s		77.4 K	90.2 K	193 K	273 K
	α(experimental) [26,27]	4.1	4.3	6.2	7.7
	α(D = 20 K; $c\theta_D b$ = 50 KÅ)	3.2	3.9	7.6	8.8
	α(D = 60 K; $c\theta_D b$ = 63 KÅ)	3.6	4.3	6.6	7.4
Ne/Na: T_s		78 K	90 K	195 K	298 K
	α(experimental) [26,27]	6	6.5	12	20
	α(D = 80 K; $c\theta_D b$ = 28 KÅ)	12	12	12	12.5
	α(D = 240 K; $c\theta_D b$ = 50 KÅ)	10.2	9.2	11.7	13.0
Ne/K: T_s		77.4 K	90.2 K	193 K	273 K
	α(experimental) [26,27]	6.7	7.1	12	17.8
	α(D = 80 K; $c\theta_D b$ = 33 KÅ)	6.6	8.6	12.5	13.7
	α(D = 240 K; $c\theta_D b$ = 50 KÅ)	7.5	7.2	9.4	11.8
Ar/K: T_s		77.4 K	90.2 K	193 K	273 K
	α(experimental) [26,27]	48	43.5	38.6	44
	α(D = 300 K: $c\theta_D b$ = 18 KÅ)	50	47	36	32
	α(D = 950 K; $c\theta_D b$ = 45 KÅ)	46	43	32	30

[a] All values of α are multiplied by 100.

Figure Captions

Fig. 1. Geometry of an individual collision. The surface is represented by an array of cubical atoms on springs. The gas atom, approaching at angle θ to the surface normal, is accelerated in the normal direction and begins its interaction with a single atom while moving at angle θ'. During the collision its momentum parallel to the surface is conserved; but that in the normal direction is altered. Depending on the size of the exchange, the gas atom may rebound (dashed line) or hop and possibly be trapped on the surface (dotted line).

Fig. 2. Equilibrium ($T_s = T_g = T$) accommodation coefficients for neon on tungsten. Crosses indicate experimental measurements [23,26,27]; for temperatures of 450 K and 600 K, their vertical heights indicate the spread of experimental results. The solid lines represent computed values using the hopping case with parameter values $D = 240$ K, $c\theta_D b = 50$ KÅ and $D = 400$ K, $c\theta_D b = 65$ KÅ labelled by the value of D. The dashed lines represent the best-fit results for the nonhopping case with $D = 240$ K, $c\theta_D b = 38$ KÅ and $D = 400$ K, $c\theta_D b = 50$ KÅ.

Fig. 3. Equilibrium accommodation coefficients for helium on tungsten. Crosses represent experimental data for ^{4}He on tungsten, and the vertical arrows represent measured differences between ^{3}He and ^{4}He on tungsten [7,23,26,27,28,29,30,31]. The solid curves represent calculated values for ^{4}He for the cases $D = 60$ K, $c\theta_D b = 60$ KÅ and $D = 100$ K, $c\theta_D b = 75$ KÅ. The dashed curves represent calculated values for ^{3}He for the cases $D = 60$ K, $c\theta_D b = 60$ KÅ and $D = 100$ K, $c\theta_D b = 75$ KÅ.

Fig. 4. Equilibrium accommodation coefficients for argon, krypton, and xenon on tungsten. Experimental data [23,26,27] are represented by the symbols: Ar = +, Kr = o, Xe = x. The computed fits, represented by the solid curves, correspond to the following parameter choices: Ar, $D = 950$ K, $c\theta_D b = 43$ KÅ; Kr, $D = 2250$ K, $c\theta_D b = 46$ KÅ; Xe, $D = 4250$ K, $c\theta_D b = 43$ KÅ.

Fig. 5. The correction factor c. Results from the best computed fits to experimental data are plotted. For the noble gases on alkali metals, two fits are given ⊙ and ⊡ corresponding to the plausible range of the parameter D. Figures 5a and 5b correspond respectively to typical gas energies of 300 K and 600 K respectively. The correlation of c with t_c/t_e is evident in a and b, whereas no correlation of c with μ is observed for $\mu < 1$ in 5c.

Fig. 6. Hydrogen molecules on graphite. Values for the equilibrium ($T_g = T_s$) accommodation coefficient α (solid line) and trapping fraction f_t (dashed line), computed with parameter values discussed in the text, are given. Experimental values for α are indicated by x [19].

Fig. 7. Dependence of the accommodation coefficient on mass ratio μ. The curves are labelled with the corresponding values of $T_g/D = T_s/D$, except for the heavy solid line labelled "fp," which represents the result for free-particle interactions. The groups of curves represent different values for K: solid lines, K = 1.0; dashed lines, K = 0.32, dash-dotted lines, K = 0.1.

Fig. 8. Dependence of the accommodation coefficient on the parameter K. Curves are labelled by the corresponding value of the ratio T_g/D. The curves presented are for $T_s/D = 0.1$ but are relatively insensitive to T_s/D as is illustrated in the figs. 9b and 9c. The two groups of curves correspond to different values of mass ratio: solid curves represent $\mu = 0.455$ while dashed curves represent $\mu = 0.11$.

Fig. 9 Dependence of accommodation coefficient on surface temperature. Curves are labelled with the corresponding value of the ratio T_g/D. Different groups of curves correspond to different values of K: solid curves, K = 1.0; dashed curves, K = 0.32; dot-dashed curves, K = 0.1. The mass ratio if $\mu = 0.022$ in fig. 9a and 0.11 in fig. 9b.

Fig. 10. Definition of coordinates describing a collision. The corresponding dimensionless parameters χ and η are given in the parentheses.

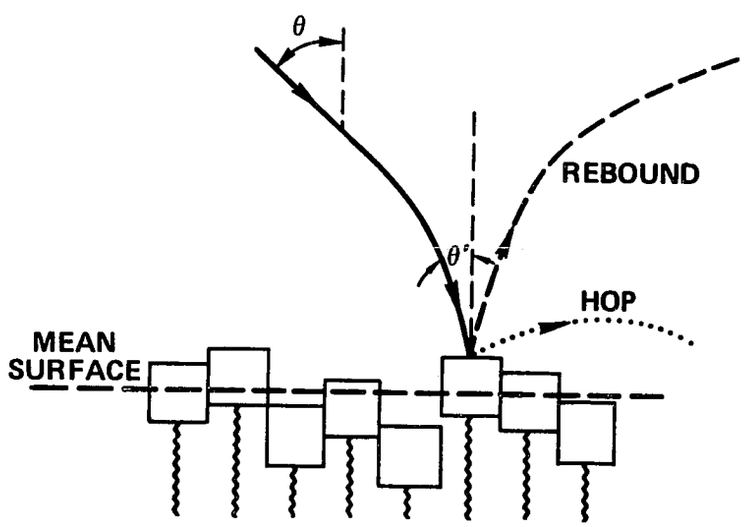

Fig. 1

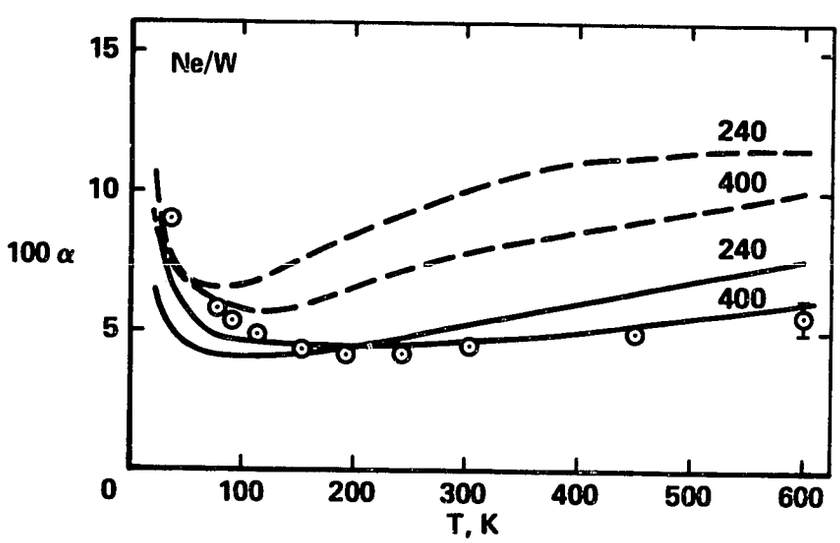

Fig. 2

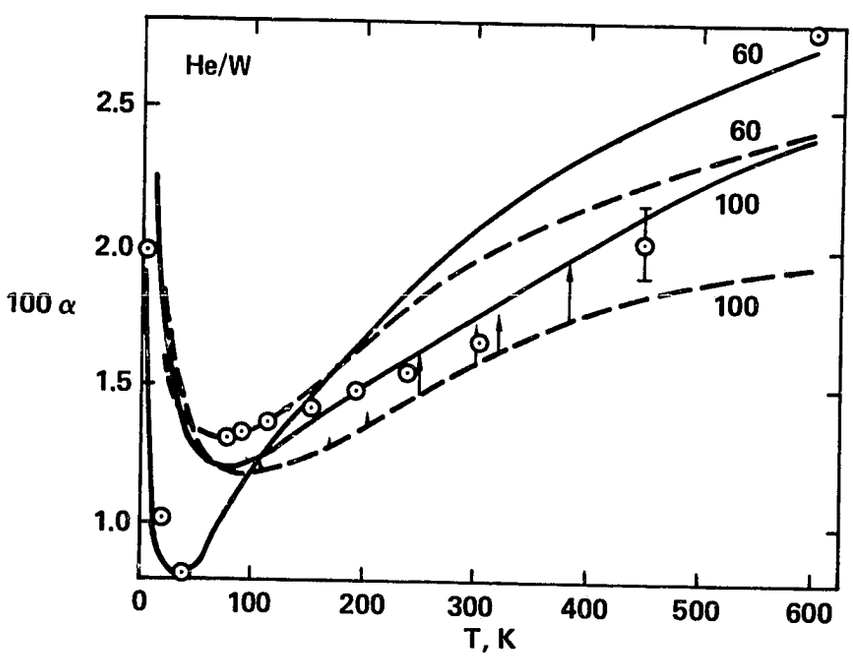

Fig. 3

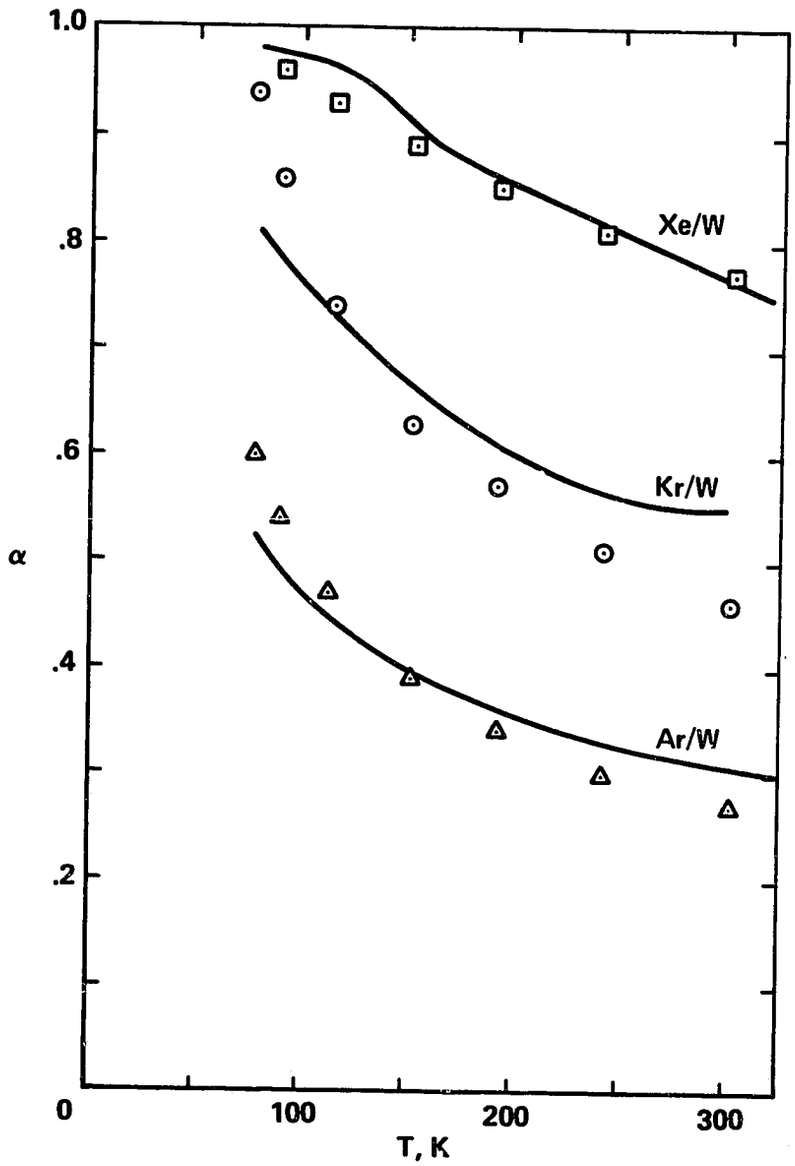

Fig. 4

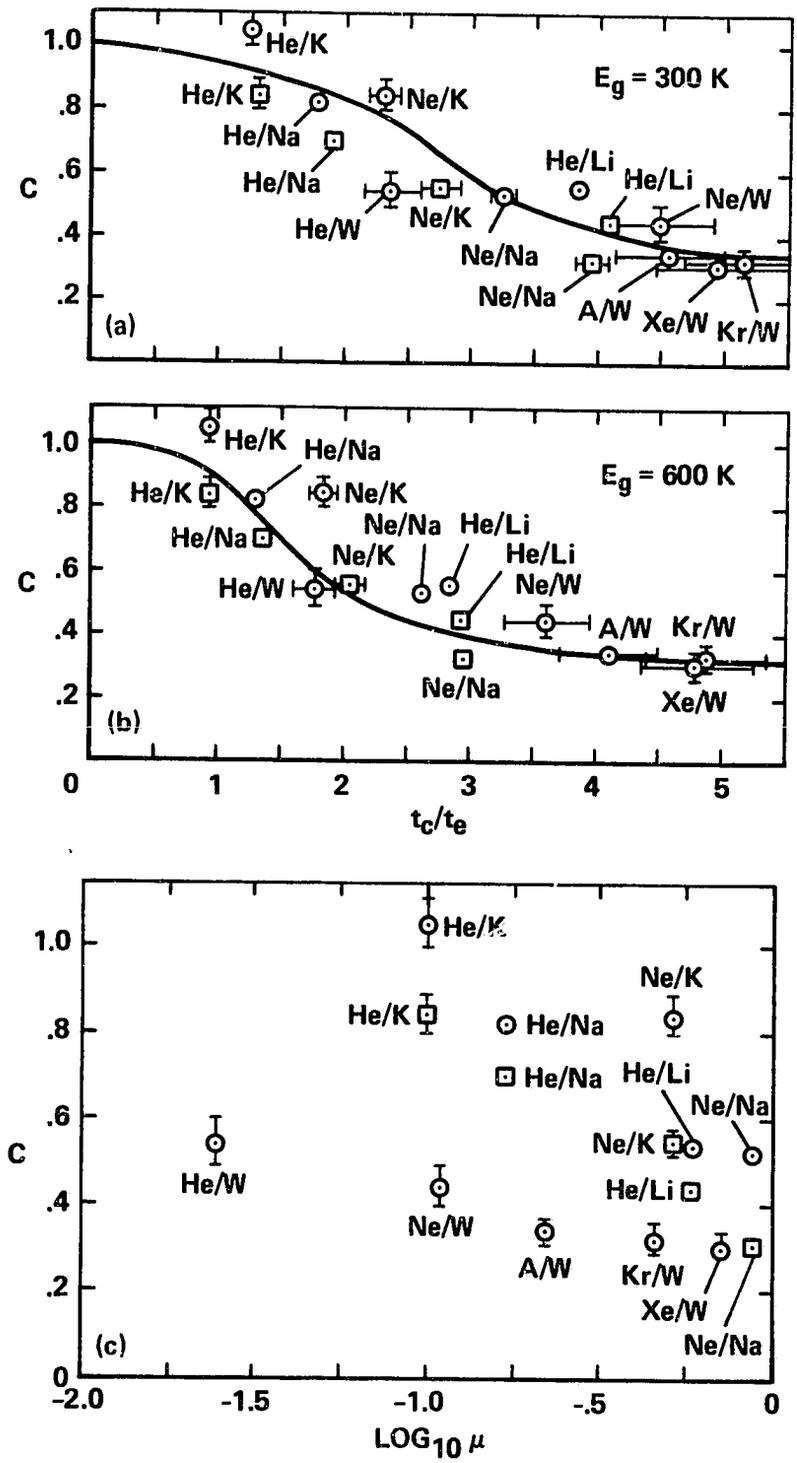
1.0
.8
.6
.4
.2
C
He/K
He/K
He/Na
He/Na
He/W
Ne/K
Ne/K
Ne/Na
Ne/Na
He/Li
He/Li
Ne/W
A/W
Xe/W
Kr/W
E_g = 300 K
(a)
He/K
He/Na
He/K
Ne/K
He/Na
Ne/K
He/W
Ne/Na
He/Li
He/Li
Ne/W
A/W
Kr/W
Ne/Na
Xe/W
E_g = 600 K
(b)
0
1
2
3
4
5
t_c/t_e
He/K
He/K
Ne/K
He/Na
He/Na
He/Na
He/Li
Ne/Na
Ne/K
He/W
He/Li
Ne/W
Ne/K
He/Li
Ne/Na
He/W
Ne/W
A/W
Kr/W
Xe/W
Ne/Na
(c)
-2.0
-1.5
-1.0
-.5
0
$LOG_{10}\,\mu$

Fig. 5

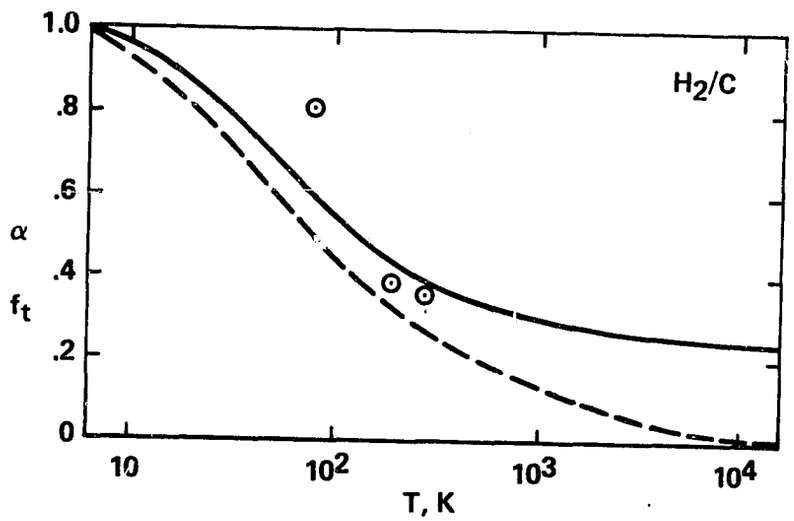

Fig. 6

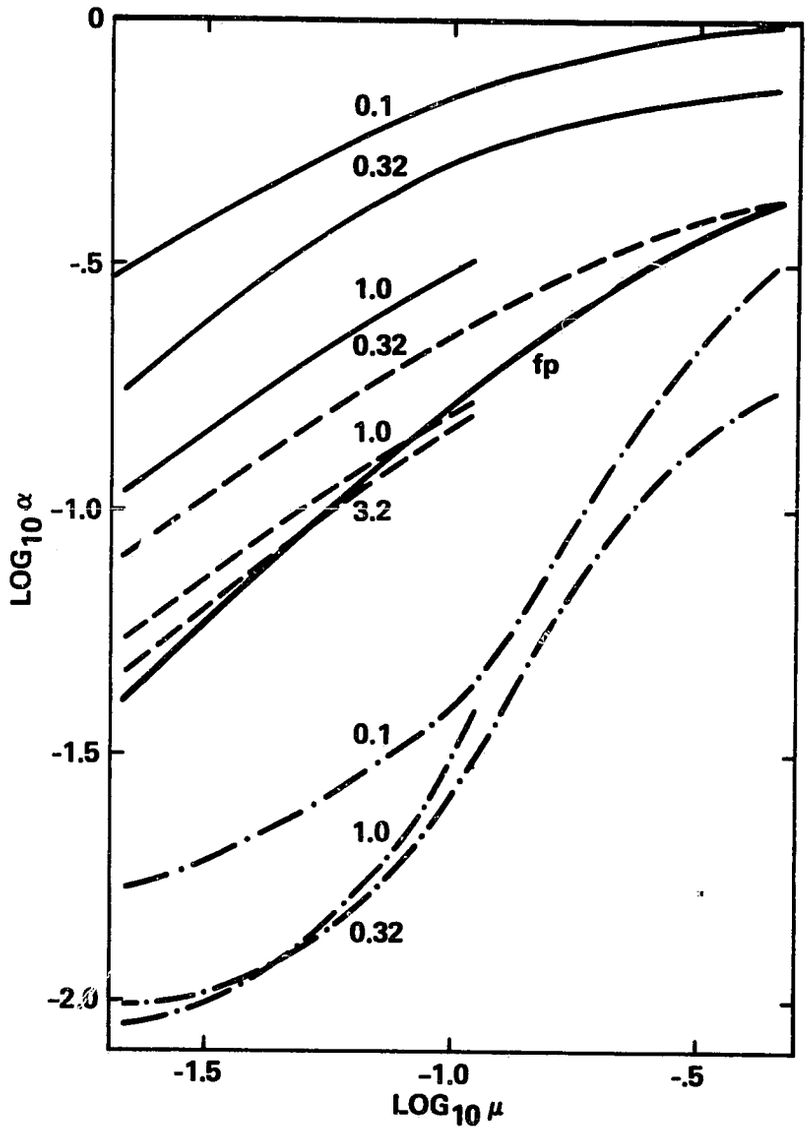
0
-.5
-1.0
-1.5
-2.0
$LOG_{10}\alpha$
0.1
0.32
1.0
0.32
fp
1.0
3.2
0.1
1.0
0.32
-1.5
-1.0
-.5
$LOG_{10}\mu$

Fig. 7

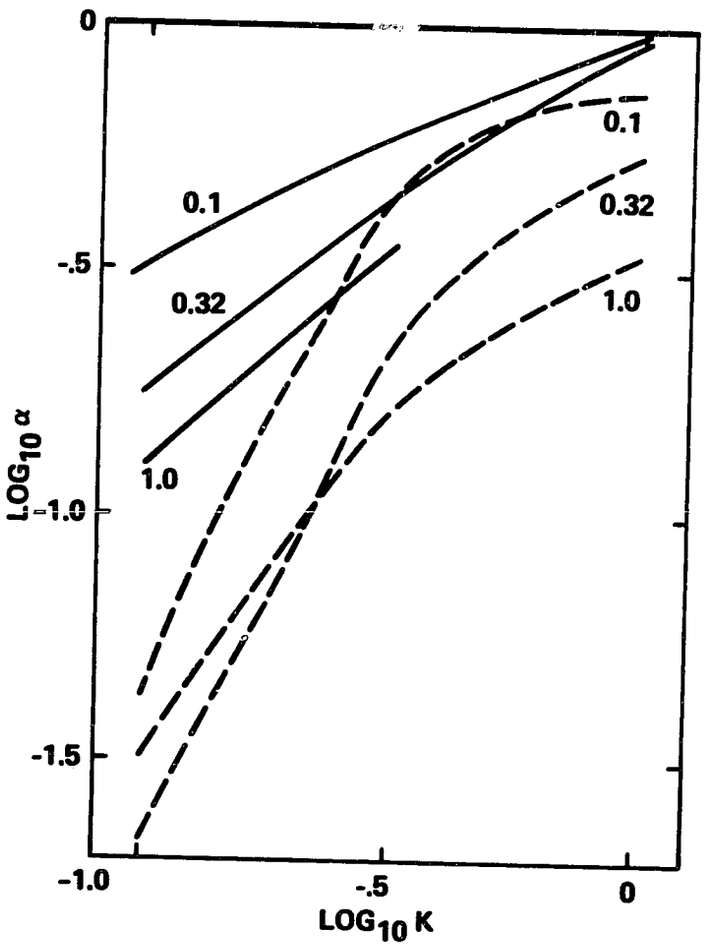

Fig. 8

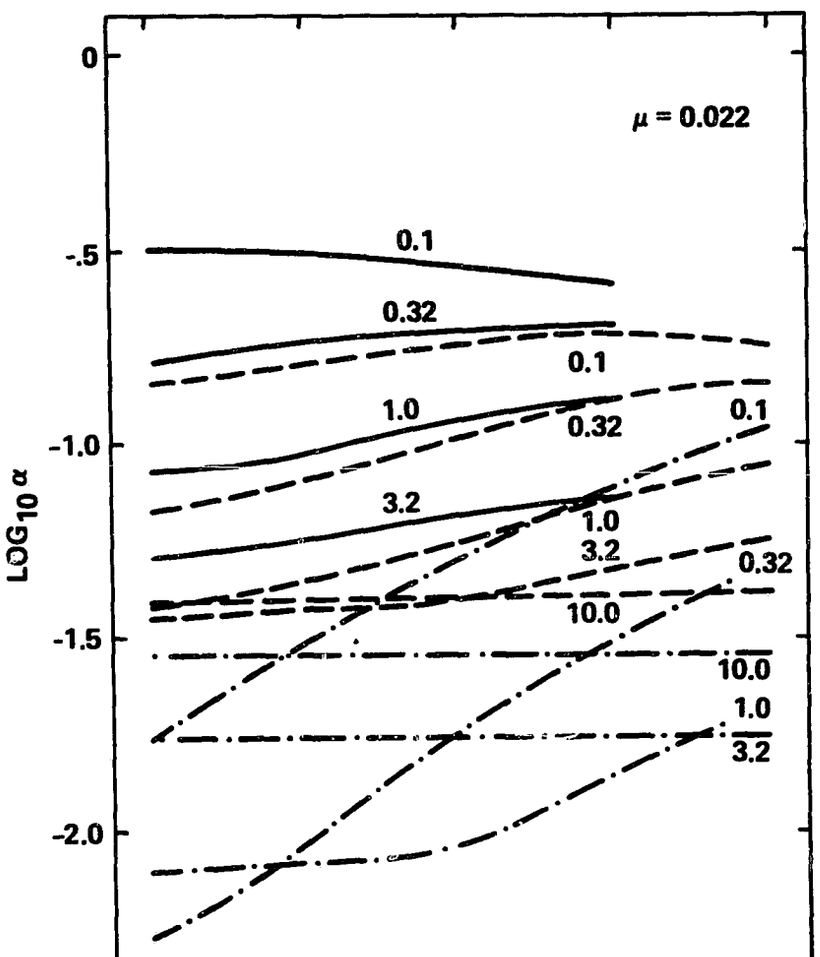
0
-.5
-1.0
-1.5
-2.0
$\mu = 0.022$
0.1
0.32
0.1
1.0
0.32
0.1
3.2
1.0
3.2
0.32
10.0
10.0
1.0
3.2
$LOG_{10}\,\alpha$
-1.0
-.5
0
.5
1.0
$LOG_{10}\,T_s/D$

Fig. 9a

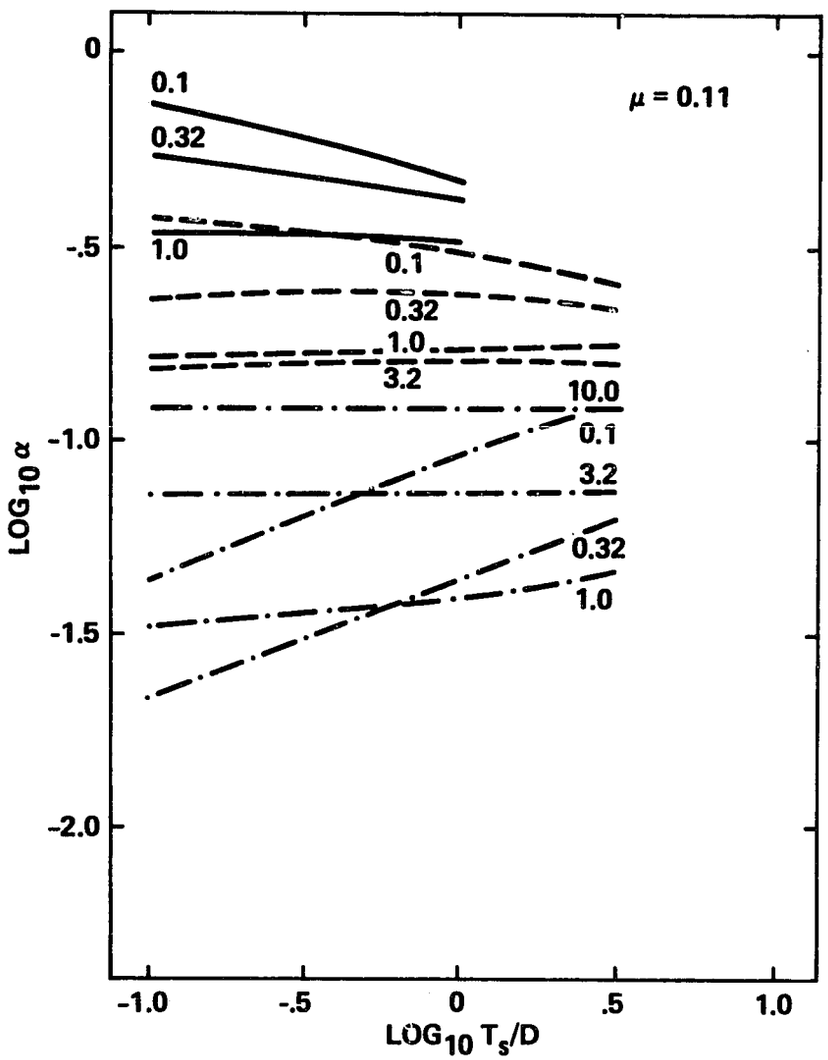
0
-.5
-1.0
-1.5
-2.0
$LOG_{10}\alpha$
$\mu = 0.11$
0.1
0.32
1.0
0.1
0.32
1.0
3.2
10.0
0.1
3.2
0.32
1.0
-1.0
-.5
0
.5
1.0
$LOG_{10}\ T_s/D$

Fig. 9b

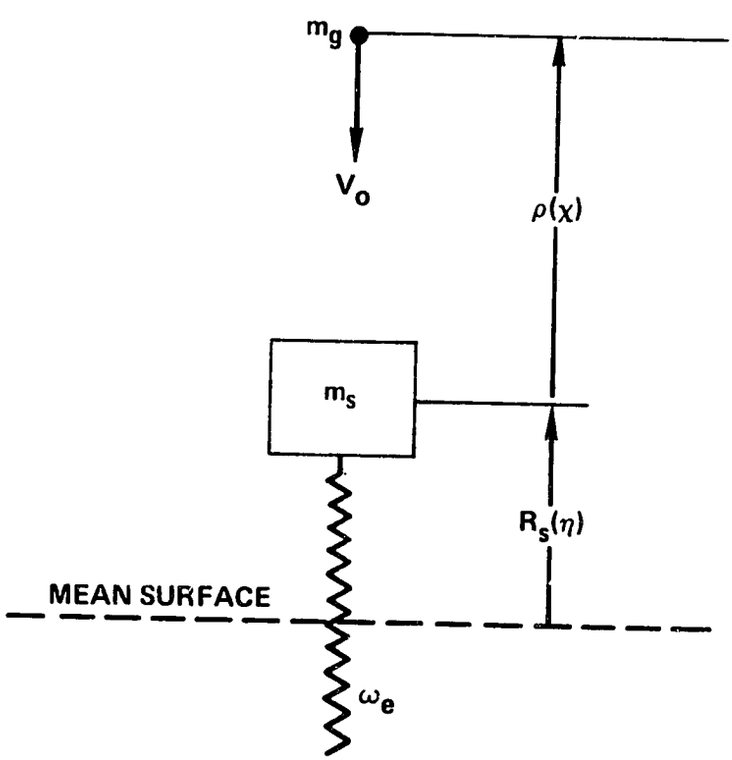

Fig. 10